Integrated analysis of single-cell and bulk RNA-sequencing identifies a signature based on macrophage marker genes involved in prostate cancer prognosis and treatment responsiveness

Xiugai Li
Department of Epidemiology, School of Public Health, China Medical University
Chang Zheng
Department of Clinical Epidemiology and Center of Evidence-Based Medicine, The First Affiliated Hospital, China Medical University
Xiaoxia Xue
Science Experiment Center, China Medical University
Junying Wu
Department of Epidemiology, School of Public Health, China Medical University
Fei Li
Department of Epidemiology, School of Public Health, China Medical University
Dan Song
Department of Epidemiology, School of Public Health, China Medical University
Xuelian Li (xlli@cmu.edu.cn)
Department of Epidemiology, School of Public Health, China Medical University

Research Article

Keywords: Prostate cancer, Macrophage marker genes, Tumor microenvironment, Treatment response, Prognosis

Posted Date: October 5th, 2022

DOI: https://doi.org/10.21203/rs.3.rs-2116772/v1

Abstract

Background

In the tumor microenvironment, tumor-associated macrophages (TAMs) interact with cancer cells and contribute to the progression of solid tumors. Nonetheless, the clinical significance of TAMs-related biomarkers in prostate cancer (PCa) is largely unexplored. The present study aimed to construct a macrophage-related signature (MRS) for predicting the prognosis of PCa patients based on macrophage marker genes and exploring its potential mechanisms.

Methods

Six cohorts containing 1056 PCa patients with RNA-Seq and follow-up data were enrolled in this study. Based on macrophage marker genes identified by single-cell RNA-sequencing (scRNA-seq) analysis, univariate analysis, least absolute shrinkage and selection operator (Lasso)-Cox regression, and machine learning procedure were performed to derive a consensus MRS. The receiver operating characteristic curve (ROC), concordance index, and decision curve analyses were used to confirm the predictive capacity.

Results

The predictive performance of MRS for recurrence-free survival (RFS) is stable and robust, and it outperforms traditional clinical variables. Furthermore, the high MRS patients presented abundant macrophage infiltration and high expression of immune checkpoint genes (CTLA4, HAVCR2, and CD86). The frequency of mutations was relatively high in high MRS group. However, the low MRS patients indicated a better response to immune checkpoint blockade (ICB) and leuprolide-based adjuvant chemotherapy. Notably, the abnormal ATF3 expression may be associated with docetaxel and cabazitaxel-resistant in the PCa cell lines.

Conclusions

In this study, a novel MRS was first developed and validated to accurately predict patients' RFS, assess immune characteristics, infer therapeutic benefits, and provide an auxiliary tool for personalized therapies.

Introduction

Prostate cancer (PCa) is the world's second most diagnosed cancer type and the leading cause of cancer-related deaths in men [1]. Currently, radical prostatectomy (RP) and radiotherapy with or without androgen deprivation therapy (ADT) remain the standard therapeutic regimen for clinically localized PCa

[2, 3]. Although most PCa patients respond to treatment initially, many eventually progress to castration-resistant prostate cancer (CRPC) or neuroendocrine prostate cancer (NEPC) [4]. The rate of biochemical recurrence (BCR) following RP was estimated to be 17–33% [5, 6]. BCR may predict disease recurrence and subsequent lethal metastases, but BCR often predates other signs of clinical progression by several years [7]. Hence, there is an urgent need to determine biomarkers that predict potential recurrence before therapy. Most studies have focused on investigating cell-autonomous alterations in CRPC, while the contributions of the tumor microenvironment are less understood. TAMs are the most abundant immune subpopulation in various malignancies, especially PCa [8–10]. The tumor-promoting M2 phenotype often outweighs the cytotoxic M1 phenotype and is used to reflect the clinical features of advanced PCa [11]. TAMs are known to promote tumor growth and resistance to therapy by releasing cytokines, inhibiting immune surveillance, enhancing angiogenic mediators, and other mechanisms [12, 13]. Mechanistically, macrophage-derived CCL5 can mediate the STAT3-dependent epithelial-mesenchymal transition process, causing drug resistance and metastasis in PCa [14]. research has shown that CSF1R inhibitors contribute to the therapeutic resistance of PCa as a macrophage targeting agent [15].

Nowadays, the growing research on scRNA-seq has led to the identification of a multitude of potentially predictive biomarkers in PCa, exploring tumor heterogeneity and mechanisms, effectively [16, 17]. Furthermore, studies have found that a signature based on B cell marker genes for lung adenocarcinoma could effectively predict patients' survival and immunotherapy [18]. Given the importance of TAMs in anti-tumor immunity, it is necessary to incorporate molecular characteristics of immune cells and their associations with prognosis and immunotherapeutic prediction into preclinical models.

Here, a novel MRS model is developed and validated using six independent public datasets to predict patients' prognosis, recurrence, as well as immune characteristics, drug sensitivity, and immunotherapy response. The relationship between this model and the advantages of leuprolide-based adjuvant chemotherapy (ACT) was analyzed, and drug sensitivity in PCa was assessed. This study may facilitate individualized treatment strategies and provide new perspectives for cancer immunity.

Materials And Methods

1. Curation and preprocessing of public datasets

The genomic expression and matched clinicopathological annotations of prostate cancer samples were retrieved from The Cancer Genome Atlas Prostate Adenocarcinoma (TCGA-PRAD) (https://portal.gdc.cancer.gov/) and the Gene Expression Omnibus database (GEO) (https://www.ncbi.nlm.nih.gov/geo/) [GSE116918, GSE70768, GSE70769, GSE46602 and GSE21032/Memorial Sloan Kettering Cancer Center (MSKCC)]. Moreover, single-cell RNA-seq data of three PRAD samples of GSE153892 were employed to identify macrophage marker genes in different cell clusters. Next, the microarray data of PCa cell lines were downloaded from three drug-related datasets (GSE36135-GPL571, GSE33455, and GSE158494) to assess important gene expressions in docetaxel and cabazitaxel samples.

Then, all counts or fragments per kilobase of transcript per million (FPKM) values were converted to transcripts per kilobase million (TPM) values and were directly used for further analysis. Probe IDs are mapped to gene symbols according to the corresponding annotation GENCODE (Homo sapiens GRCh38). The probes with the same gene were expressed as average values. Finally, a total of 1056 patients with available clinical information were included in subsequent analysis, integrated by the "ComBat" algorithm, which eliminates potential batch effects across datasets. The baseline information of collected cohorts was provided in Supplementary Table 1.

2. Distinguishing and extraction of macrophage marker genes

The scRNA-seq analysis was conducted by using the "Seurat" and "SingleR" packages [19, 20]. All other parameters were run with default values. Cells with more than 5% of the mitochondrial gene were removed. Principal component analysis (PCA) dimensionality reduction was performed using 2000 highly variable genes and the top 10 principal components were selected for cell clustering analysis based on the “tsne” package in R. The |log2FC| > 0.25 and adjusted P-value < 0.05 were set as the thresholds for identifying marker genes.

3. Development of the MRS signature

Machine learning algorithms, including Lasso [21], stepwise Cox, random survival forest (RSF) [22], generalized boosted regression modeling (GBM), partial least squares regression for Cox (plsRcox), CoxBoost, survival support vector machine (survival-SVM) and supervised principal components (SuperPC) were integrated to build a consensus signature. Using the “survival” and “survminer” packages to fit univariate cox regression in the meta cohort, the P-value of 0.05 was considered RFS-associated genes. The Lasso method was performed via the glmnet package, where all crossover mRNAs were penalized for preventing over-fitting. The above analysis was adopted to better choose stable hub genes. Consequently, we employed integrative algorithms to establish a predictive model based on the leave-one-out cross-validation (LOOCV) framework in the TCGA-PRAD cohort and applied all models to five validation cohorts (GSE116918, GSE70768, GSE70769, GSE46602, and MSKCC). After calculating Harrell’s concordance index (C-index) across all validation cohorts, the optimal model was selected according to the highest average C-index.

4. Somatic mutation profile analysis

According to mutation data of TCGA-PRAD samples, we calculated tumor mutational burden (TMB) using “Maftools” to compare the relationship between TMB and MRS scores. Additionally, oncoprint plots displayed differences in the frequency of alterations between high/low MRS subgroups. The microsatellite instability (MSI) was inferred using the PreMSIm method.

5. Evaluation of the immunological characteristics

With transcriptome-based algorithms, ESTIMATE [23] compute the immune/stromal scores to reflect the overall immune infiltration, and single-sample gene set enrichment analysis (ssGSEA) [24] and

CIBERSORT [25] were employed to quantify the relative immune cell proportions. Additionally, the 20 immune checkpoint molecules were retrieved from studies by Auslander et al. [26] and Hu et al. [27]. The immunotherapy responses in PCa patients were inferred by the tumor immune dysfunction and exclusion (TIDE) score.

6. Functional Enrichment Analysis

Gene annotation enrichment analysis was performed using the “clusterProfiler” and “fgsea” packages. Differentially expressed genes (DEGs) were identified with a threshold of |log2 FC| > 1 and P < 0.05 by the R package “limma”, and also clustered into various Kyoto Encyclopedia of Genes and Genomes (KEGG) pathways and biological processes of Gene Ontology (GOBP). Using the file (msigdb.v7.4.symbols.gmt) as a reference, gene set enrichment analysis (GSEA) was performed using the GSEA software to analyze various potential signaling pathways. The biological pathways were significantly enriched when nominal P-value (NOM P-value) < 0.05 and FDR < 0.25 after 1000 permutations. Protein-protein interaction (PPI) networks were generated using “STRINGdb” package to describe the interactions among representative DEGs and visualized using Cytoscape (3.8.2).

7. Prediction of therapeutic sensitivity

A total of 2,191 compounds from three drug sensitivity databases (GDSC2, CTRPv2.0, and PRISM), which accessed via the Cancer Dependency Map (DepMap) portal (https://depmap.org/portal/). The lower IC50 (or AUC) value represents a higher sensitivity to compounds. The IC50 (or AUC) of each compound was predicted by the calcPhenotype function of “pRRophetic” package. The correlation between IC50, AUC values, and MRS scores for prostate cancer was evaluated via the Pearson correlation analysis (GDSC: $r < -0.29$; CTRP: $r < -0.39$; PRISM: $r < -0.35$;). Box plots were depicted to assess the differential drug response of the signature.

8. Statistical analysis

All statistical analyses were conducted using R (4.2.1). The Kaplan-Meier (KM) and log-rank tests were applied to detect the survival difference. The optimal cutoff value was defined using the “survminer” algorithm. The comparison of the C-index with different models was carried out using the CompareC package. The ROC and Area under the ROC curve (AUC) were used to explore exactly the predictive ability, which was drawn via pROC and timeROC packages. Heatmaps were generated using the R package “ggcor”. Decision Curve Analysis (DCA) captured the clinical efficacy when we try to use complex models as a tool for decision-makers [28, 29]. Using the Pearson analysis to evaluate the corresponding coefficients between two continuous variables. Wilcox test or Kruskal-Wallis or Student’s t-test was employed to compare differences between groups. The chi-squared test was applied for categorical variables. P-value or adjusted P-value less than 0.05 were regarded as statistically significant.

Results

1. Identification and selection of macrophage marker gene expression profiles

Figure 1 depicts the complete work framework of this study. The clinicopathological features of TCGA cohorts are presented in Table 1. In this study, 1056 PCa patients were included in a large meta-cohort, and the cross-platform batch effect was first removed using ComBat. Following the removal, the clustering across platforms was closer than before (Fig. 2A, B). After data processing and filtering, three PCa samples were extracted from the GSE153892, and the gene expression profile of 11,527 cells was identified for subsequent analysis. The plots showed the distribution and dissimilarity of the ten cell clusters (Fig. 2C, D). Cellular annotations for each cluster were determined by cross-referencing DEGs with typical marker genes, and cells in cluster 5 were classified as macrophage cells (Fig. 2E). As a result, 447 macrophage marker genes of PCa were identified. Subsequently, 329 genes were obtained from the meta cohort.

Table 1
Baseline clinical characteristic of TCGA Database

Characteristics	Low MRS (N = 371)	High MRS (N = 58)	P-value
Age, median (IQR)	61 (56,66)	63 (57,66)	0.24
T stage	6 missing		< 0.001
T2	151(35.70%)	3(0.71%)	
T3	210(49.65%)	51(12.06%)	
T4	5(1.18%)	3(0.71%)	
N stage	55 missing		< 0.001
N0	272(72.73%)	33(8.82%)	
N1	49(13.10%)	20(5.35%)	
Biochemical recurrence			< 0.001
No	346(80.65%)	25(5.83%)	
Yes	25(5.83%)	33(7.69%)	
Gleason score			< 0.001
GS = 6–7	232(54.08%)	12(2.80%)	
GS = 8–10	139(32.40%)	46(10.72%)	
Residual tumor	148 missing		< 0.001
No	212(75.44%)	27(9.61%)	
Yes	27(9.61%)	15(5.34%)	
Response to ACT	55 missing		< 0.001
No	297(79.41%)	30(8.02%)	
Yes	30(8.02%)	17(4.55%)	

*IQR, interquartile range

2. Integrative construction of the MRS model

Based on 329 macrophage genes from the meta cohort, univariate analysis was used to screen 104 prognostic genes with P < 0.05 (Supplementary Table 2). Then, Lasso-Cox analysis was performed to acquire 40 more stable genes that were significantly associated with RFS in PCa patients. Finally, these genes were selected for the machine learning-based integration procedure to develop a consensus MRS.

In the TCGA-PRAD dataset, we fitted nine prediction models through the LOOCV framework and then calculated the C-index of each model in the other five validation datasets (Fig. 3A). Interestingly, the average C-index (0.699) was highest in the RSF model and higher in most validation datasets (Supplementary Table 3). Meanwhile, the optimal cut-off value was confirmed to be 13.45. PRAD samples were categorized as low and high MRS subgroups based on the value. The survival curve in the TCGA-PRAD training dataset indicated that high MRS patients had a significantly inferior RFS ($P < 0.001$) (Fig. 3B). Furthermore, similar trends were detected in the five validation datasets and meta-cohort combining all samples and performed well (Fig. 3C-H).

3. Prognostic assessment of the signature

The estimated AUC value for 1-, 3-, and 5-year survival rates were 0.854, 0.902, and 0.925 in TCGA-PRAD (Supplementary Fig. 1A); 0.754, 0.781, and 0.763 in MSKCC (Supplementary Fig. 1B); 0.975, 0.617, and 0.680 in GSE116918 (Supplementary Fig. 1C); 0.709, 0.756, and 0.609 in GSE70768 (Supplementary Fig. 1D); 0.688, 0.754, and 0.816 in GSE46602 (Supplementary Fig. 1F); 0.834, 0.851, and 0.887 in Meta-cohort (Supplementary Fig. 1G), respectively. The AUC values for 3-, 4-, and 5-year survival rates were 0.832, 0.874, and 0.816 in GSE70769, respectively (Supplementary Fig. 1E). These findings suggested that the MRS model had significant predictive power. The performance of MRS was further compared with other clinicopathological features in predicting prognosis. MRS had distinctly favorable accuracy than other variables, including age; T, prostate-specific antigen (PSA) level, Gleason score, TMB, and MSI. (Fig. 4A-F). However, there was no difference in MSKCC datasets. Next, the MRS performance was assessed in the TCGA cohort to further evaluate its clinical utility. DCA analysis indicated that the MRS model added more net benefit than the clinical characteristics. It also indicated that prediction with all or non-patient schemes is more beneficial when the decision probability based on the nomogram is greater than 0.1 and less than 0.3 (Fig. 4G). The findings also revealed that the combination of MRS and pathologic parameters might improve superior clinical usefulness for PCa patients.

4. The immune landscape of MRS subgroups

We used the GSEA algorithm to enrich the various signal pathways in the meta cohort to better understand the underlying mechanisms associated with MRS in PCa. Signaling pathways such as cell cycle and DNA replication were specifically active in the high MRS subgroup. In contrast, the metabolic pathways were significantly enriched in the low MRS subgroup, including drug metabolism cytochrome p450, adipocytokine signaling pathway, and peroxisome (Supplementary Fig. 2A). Simultaneously, GOBPs analysis was performed, and the results suggested that most genes were significantly associated with five pathways ($P < 0.05$), such as regulation of cell development, ameboid-type cell migration, positive regulation of MAPK cascade, positive regulation of cell adhesion, and small molecule catabolic process (Supplementary Fig. 2B). Particularly, a thorough search of the TCGA training dataset revealed that 313 DEGs ($|LogFC| > 1$ and $P < 0.05$) were involved in multiple KEGG immune-related pathways, such as IL-17 signaling pathway, TNF signaling pathway, MAPK signaling pathway, Human T-cell leukemia virus 1 infection, Cytokine-cytokine receptor interaction, and PI3K-Akt signaling pathway. Then, based on

the STRING database, the PPI network was generated to reveal interactions among representative DEGs (containing 46 proteins), which regulated the immune response to a specific level (Fig. 5A). In addition to the enrichment differences observed above, the relationship between the MRS and immune cell and checkpoints in meta PCa samples was investigated.

The immune, stromal, and estimate scores were positively correlated with MRS, while tumor purity had significant negative dependencies (Fig. 5B, C; Supplementary Fig. 2C, D). Furthermore, CIBERSORT analysis displayed that PCa patients with high MRS had a significantly greater proportion of memory B cells, resting memory CD4 T cells, regulatory T cells (Tregs), gamma delta T cells, activated NK cells, and M1/M2 macrophages, but had a lower proportion of plasma cells and T follicular helper cells (Fig. 5D). Simultaneously, a correlation heatmap was generated to illustrate the relationships among MRS and 28 different immune cells from ssGSEA. The Pearson analysis was performed in all types of immune cells, and 13 pairs exhibited significantly positive correlations, especially among memory B cells and gamma delta T cells, while activated B cells, CD56 bright natural killer cells, eosinophils, immature dendritic cells, mast cells, and natural killer cells were negatively correlated. Besides, the correlation between the expressions of 20 genes (15 immune checkpoint-related genes and 5 immunological activity-related genes) and MRS were analyzed. Moreover, this analysis suggested that 12 genes were positively correlated with MRS, and CEACAM1, CD40, and PVR were negatively correlated (Fig. 5E). Violin plots also suggested that 11 immune cells were highly infiltrated in the high MRS group which exhibited a positive correlation with MRS (Supplementary Fig. 2E). Moreover, the expression of most checkpoints was upregulated in the high MRS group, which may be associated with overall upregulation of immune activity. Details of the expression patterns of genes are depicted in Supplementary Fig. 2F. These genes were all positively correlated with MRS scores.

Due to suppression of critical immune checkpoints can influence cancer immunotherapy with ICB, some representative molecules (CTLA4, HAVCR2, and CD86) were evaluated, and it was observed that they had a positive correlation with MRS. The patients were categorized into four subtypes based on MRS and checkpoint genes and the impact of their interaction on RFS in PCa patients was determined using the KM curve. The log-rank test results showed that MRS could effectively differentiate the prognosis of patients with conflicting levels of CTLA4 (Fig. 5G), HAVCR2 (Fig. 5H), and CD86 (Fig. 5I). Patients with the worst prognosis had low MRS scores and high expressions of checkpoints, while patients with high MRS scores and low expressions of checkpoints had the highest survival rates among the four subtypes. Hence, we hypothesized that it might be used to predict immunotherapeutic response in PCa. The Wilcoxon test results also demonstrated that tumors with low MRS scores had significantly lower TIDE score, implying a better response to ICB therapy (Fig. 5F). Overall, these findings demonstrated that MRS correlated with immune activation and indicated potential ICB benefits in PCa.

5. Somatic Mutation characteristics were observed in different MRS groups

Increasing evidence suggests that high mutational load and neoantigen overexpression increase the chances of tumor recognition by the immune system [30]. Therefore, the maftools approach was used in the present study to investigate the possible relationship between mutational load and MRS scores. First, Using the MRS score, patients were classified into two groups (low and high). The oncoPrint plots summarized the top 10 mutated genes in the high MRS groups (31%, 14%, 10%, 10%, and 10% for TP53, TTN, ABCA13, CSMD3, and FOXA1 respectively) (Fig. 6A). The mutation rates for SPOP, TTN, TP53, FOXA1, and KMT2D in the low MRS subgroup were 12%, 9%, 8%, 5%, and 5%, respectively. Also, the forest plot showed that ABCA13 was highly mutated in the high MRS group (Fig. 6B). Subsequently, a series of evaluation indicators such as TMB, MSI, and immune checkpoint molecule expression represented the responsiveness to immunotherapy. The findings suggested that CD86, CTLA4, HAVCR2, PDCD1LG2, and CXCL9 expression levels were significantly elevated as MRS increased, and TMB scores were significantly distributed in the high MRS group (Supplementary Fig. 2F, Fig. 6C). The MRS score in MSI-L/MSS was higher than in MSI-H (Fig. 6D). These results demonstrated that MRS might correlate with higher immunogenicity and heterogeneity in PCa.

6. Potential therapeutic compounds of PCa patients with high MRS

Many studies have been searching for potential druggable targets and compounds for PCa patients because of resistance to standard chemotherapeutic agents. In the TCGA-PRAD cohort, 21 patients were treated with leuprolide-based ACT. The chi-square test results demonstrated that the low MRS subgroup exhibited a higher response rate than the high MRS subgroup (91% vs. 50%) (Fig. 7A), and MRS could also significantly discriminate responders from non-responders of leuprolide-based ACT (AUC = 0.722) (Fig. 7B).

Next, three drug response databases (GDSC, CTRP, and PRISM) were searched to identify effective chemotherapeutic agents for patients with high MRS scores and poor prognoses. First, IC50 values were estimated for each sample in the meta-cohort, and then correlations between values and the MRS were calculated. A screening threshold of negative r values with p-values less than 0.05 was used to identify candidate compounds, with five compounds annotated with the most negative correlation coefficients displayed in volcano plots (WIKI4, MIM1, Vorinostat, GSK2578215A, and WEHI-539), and their estimated IC50 values were lower in the high MRS subgroup (Fig. 7C, D). Moreover, ten compounds were found to be negatively correlated with MRS scores, containing CD-1530, teniposide, tigecycline, LY-2183240, and leptomycin B in the CTRP database (Fig. 7E) and ixabepilone, triclabendazole, cabazitaxel, paliperidone, and SC-12267 in the PRISM database (Fig. 7G). Furthermore, the results showed that all compounds presented higher AUC values in the low MRS subgroup (Fig. 7F, H). Finally, we obtained a group of drugs from the three datasets whose beneficial therapeutic values in high MRS scores were significantly higher than low MRS scores ($p < 0.05$, Fig. 7I). Among them, vorinostat, cabazitaxel, and fludarabine have been widely used for the treatment of specific targets of PCa [31, 32].

To explore the mechanism of drug resistance, we extracted genes ranked in the top 10 of the RSF in three external datasets based on the PCa cell line and analyzed the expression differences (Supplementary Fig. 3A-C). Notably, GSE36135 and GSE33455 revealed that ATF3 expression was upregulated in docetaxel-resistant DU-145 cells respectively (Fig. 8A, B). However, the outcome was the opposite in PC-3 cells. Moreover, GSE158494 suggested that ATF3 expression was upregulated in cabazitaxel-resistant cells compared to original and docetaxel-resistant cells (Fig. 8C). According to the cutoff threshold of 2.48 derived from the expression of ATF3 in the TCGA cohort, low expression samples presented significantly poorer RFS than high expression samples ($P < 0.001$, Fig. 8D). Similarly, the expressions of ATF3 are negatively correlated with MRS scores (Fig. 8E, Supplementary Table 4).

Discussion

Macrophages have received significant attention regarding the prognosis of several cancer types [33]. Particularly, the presence of TAMs infiltration in the tumor microenvironment was associated with disease progression following ADT, and preclinical studies also recommended that TAMs promote PCa cell proliferation and migration [34–36]. The heterogeneity of PCa is being revisited with the advent of single-cell technologies. Yu et al. discovered FMO2 as a biomarker of macrophage infiltration and prognosis in epithelial ovarian cancer [37]. Additionally, MS4A6A was found to be a new prognostic biomarker produced by macrophages in glioma patients [38]. However, the underlying mechanism of TAMs-induced remains unclear, and molecular stratification of TAMs based on predictive biomarkers to guide PCa treatment selection has not been implemented in the clinic yet. Therefore, broadly exploring the prognostic markers of PCa can guide future clinical management.

In the present study, we initially identified macrophage marker genes from PRAD tissue by scRNA-seq analysis. Further, we employed univariate Cox regression analyses and Lasso to screen 40 candidate genes that were highly correlated with the RFS of patients. We further established an integrative method to generate a consensus MRS with the expression profiles of these genes. One advantage of a complex machine learning algorithm is the capacity to develop better statistical models to forecast RFS across all cohorts to enhance classification performance. A total of nine models were fitted to the TCGA-PRAD database through the LOOCV framework. Subsequently, validation results in five independent cohorts obtained from the GEO dataset suggested that RSF was the best model with the capability of stratifying PCa patients into two MRS groups. Patients with higher MRS exhibited worse RFS in the training dataset. The survival curve in five external cohorts also confirmed the good reproducibility and robustness of the MRS in predicting patients' RFS. Furthermore, the AUC value in all cohorts presented satisfying molecular subtyping accuracy. Previous studies indicated that various clinical predictors were widely used for prognostication and risk assessment of PCa, such as Gleason score, PSA, and stage [39–41]. Other parameters, such as TMB and MSI status, might potentially have an impact on therapy response and prognosis in addition to the clinicopathological features of the patient [42]. The C-index assessment suggested that the MRS signature has a significant advantage in predicting RFS relative to these factors. However, the difference showed no statistical significance in the MSKCC dataset. Notably, the decision

curve, which synthesized the MRS with clinical characteristics, added a net benefit rate to current clinical values.

Furthermore, these DEGs within subgroups were also correlated with pathways involved in inflammation, such as the IL-17 signaling pathway, TNF signaling pathway, MAPK signaling pathway, PI3K-Akt signaling pathway, Cytokine-cytokine receptor interaction, peroxisome and cell cycle. Recent studies have shown that these variables and pathways are essential for metabolic regulation and macrophage polarization [43, 44]. Next, we discovered that PCa patients with high MRS were associated with an increased risk of biochemical recurrence and had a higher immune infiltration (like Tregs, activated CD8 T cells, activated NK cells, and M1 and M2 macrophages). These observations were in agreement with the previous studies [45, 46]. We observed that higher MRS scores correlated with higher expressions of immune checkpoints (CTLA4, HAVCR2, and CD86), which, in survival studies, was shown to have a mutually beneficial influence on patient prognosis. With the increase in MRS score, the expressions of checkpoints such as CXCL9 and CD80 also increased. This might be the result of the mechanism by which M1 hot TAMs may recruit T cells through CXCL9 expression [47]. As per recent studies, overexpression of HAVCR2 in T cells can lead to dysfunction of PSA-specific CD8 + T cells, further leading to a poor prognosis for PCa patients [48, 49]. Additionally, CD80 binds to CD28 or CTLA4 to activate T cell co-stimulation or initiate T cell co-inhibition, respectively [50]. Targeting immune checkpoints was considered to improve the therapeutic efficacy of immunotherapy modalities in solid tumors [51]. This study showed that patients with low MRS benefit more from ICB treatment, but those with high TIDE scores may react poorly to immunotherapy. Therefore, the identification of MRS classifiers that predict response to immunotherapies is critical for enhancing their use in treating patients. Therefore, the mechanism about how MRS affects RFS and ICB treatment of PCa patients may require more evidences and discussions.

The high MRS subgroup presented a higher mutation frequency of TP53 (31%), and the low MRS subgroup tended to have a higher proportion of SPOP mutations (12%). Studies have reported a mutually exclusive relationship between TP53 and SPOP mutations, both of which are independent prognostic markers for CRPC [52, 53]. For example, alterations in TP53 were associated with a decreased dependence of the tumor on AR signaling, which was associated with ARSI, whereas the highest levels of AR activity were found in the SPOP mutant subtype, indicating a good response to androgen receptor signaling inhibitor (ARSI) [54]. In addition to modifying CSF1 signaling, the combination of PTEN and p53 loss increased CXCL17 secretion, further influencing macrophage recruitment and function [55, 56]. ABCA13 was highly mutated in the high MRS group. It is reported that overexpression of ABCA13 is associated with decreased progression-free survival and reduced sensitivity to temozolomide in glioblastoma [57]. Patients with microsatellite instability-high (MSI-H) responded well to immunological response [58]. This study showed a better immune response in patients with low MRS, which is in line with both the findings from the TIDE approach. However, as confirmed by various studies, the high MRS group had a higher TMB score, suggesting that TMB is unlikely to be a major determinant of response to immunotherapy for this disease [59–61]. Considering the present and previous findings, it is concluded

that the MRS score could be a credible biomarker that assists with filtering the dominant population of immunotherapy patients.

Neoadjuvant leuprolide enhances radiation-mediated apoptosis of PCa cells with well-documented effects in reducing tumor bulk and increasing progression-free survival [62]. According to this data, patients with low MRS were more inclined to respond to leuprolide-based ACT. ROC analysis suggested that MRS provided better accuracy in predicting leuprolide-based ACT. In addition, potential drug targets and corresponding compounds for high MRS PCa patients were screened as per the established MRS model, and several promising compounds were selected from three drug response databases, like paclitaxel, vorinostat, cabazitaxel, and fludarabine. It was discovered that Zn promotes the chemosensitivity of PCa cells to paclitaxel by inhibiting epithelial-mesenchymal transition and inducing apoptosis, which increases life expectancy in PCa patients [63]. Currently, Poly (ADP-ribose) polymerase inhibitors (vorinostat) can be used clinically to activate genotoxic and proteotoxic stress response pathways in human PCa [64]. Clinical trial data revealed that cabazitaxel enhanced survival with manageable side effects in patients with metastatic CRPC [65]. Furthermore, increased reactive oxygen species production by fludarabine phosphate may represent an effective treatment option for patients with N-MYC overexpressing NEPC tumors [66]. As a result, MRS might be a powerful tool for making choices for targeted drug development and immunotherapy combination for PCa patients.

Considering the impact of the tumor microenvironment on drug resistance, a differential analysis of critical genes in the external cohorts of PCa cells was performed. The GSE36135 and GSE33455 cohorts demonstrated high expression of ATF3 in docetaxel-resistant DU-145 cells compared to sensitive or original cells; however, the outcomes were opposite in the PC-3 cell line. Furthermore, GSE158494 showed that ATF3 expression was upregulated in cabazitaxel resistant cells compared to original and docetaxel resistant cells. As an inducer of oxidative stress and inflammation, ATF3 may regulate macrophage-associated host defense [67]. For example, in response to chemotherapy, wild-type macrophages exhibit pro-oncogenic activity, whereas ATF3 knockout macrophages exhibit anti-cancer activity [68]. ATF3 has been identified as a tumor suppressor for a major subset of PCa with dysfunctional PTEN and has also been shown to inhibit hormone-induced prostate carcinogenesis in mice [69, 70]. Our study further shows that the high expression of ATF3 was associated significantly with better prognosis and low MRS score. Therefore, ATF3 can be used as a key indicator of apoptosis and drug resistance in PCa cells. Although external cohorts were validated in this study, its predictive power needs further validation in prospective multicenter cohorts. Furthermore, given the complexity of the tumor microenvironment, which is influenced by multiple factors, the interaction between tumor cells and macrophage-associated genes requires more exploration and evidence. Potential drug combination interventions for MRS subgroups are expected to be further explored in clinical trials.

Conclusions

In conclusion, this study developed and validated a novel MRS by integrating machine learning algorithms to effectively predict the RFS of PCa patients. This signature presented the superior ability of

risk stratification and effectively predicted chemotherapeutic drug sensitivity and immunotherapy response, suggesting its promising future in utilization.

Abbreviations

TCGA: The Cancer Genome Atlas, GEO: Gene Expression Omnibus, PRAD: Prostate Adenocarcinoma, MSKCC: Memorial Sloan Kettering Cancer Center, TAMs: Tumour-associated macrophages, PCa: Prostate cancer, MRS: Macrophage-related signature, scRNA-seq: Single-cell RNA-sequencing, Lasso: Least absolute shrinkage and selection operator, KM: Kaplan–Meier, ROC: Receiver operating characteristic curve, AUC: Area under the ROC curve, RFS: Recurrence-free survival, Tregs: Regulatory T cells, ICB: Immune checkpoint blockade, RP: Radical prostatectomy, ADT: Androgen-deprivation therapy, ARSI: Androgen receptor signaling inhibitor, CRPC: Castration-resistant prostate cancer, NEPC: Neuroendocrine prostate cancer, BCR, Biochemical recurrence, ACT: Adjuvant chemotherapy, FPKM: Fragments per kilobase of transcript per million, TPM: Transcripts per kilobase million, PCA: Principal component analysis, RSF: Random survival forest, GBM: Generalised boosted regression modelling, plsRcox: Partial least squares regression for Cox, survival-SVM: Survival support vector machine, SuperPC: Supervised principal components, LOOCV: Leave-one-out cross-validation, C-index: Concordance index, PSA: Prostate-specific antigen, TMB: Tumor mutational burden, MSI: Microsatellite Instability, ssGSEA: Single-sample gene set enrichment analysis, TIDE: Tumor immune dysfunction and exclusion, DEGs: Differentially expressed genes, GSEA: Gene set enrichment analysis, KEGG: Kyoto Encyclopedia of Genes and Genomes, GOBP: Biological processes of Gene Ontology, GSEA: Gene set enrichment analysis, PPI: Protein–protein interaction, DCA: Decision Curve Analysis.

Declarations

Ethics approval and consent to participate

Not applicable.

Consent to publication

Not applicable.

Availability of data and materials

Publicly available datasets were analyzed in this study. This data can be found here: The data of this study were downloaded from TCGA and GEO.

Acknowledgments

The authors are grateful to everyone who has participated in this research work.

Funding information

This study was supported by the National Key Research and Development Program of China (No. 2016YFC1302500).

Author contributions

Xiugai Li: Research design, Data analysis, Original-draft, Reviewing, and Editing, Chang Zheng: Manuscript preparation, Revisions, Supervision, Xiaoxia Xue: Data analysis and Revisions, Junying Wu, Fei Li, and Dan Song: Chart preparation, Visualization, Xuelian Li: Editing, Supervision, Project administration.

Conflict of interest

The authors declare that they have no competing interests.

References

1. Vietri MT, D'Elia G, Caliendo G, Resse M, Casamassimi A, Passariello L et al. Hereditary Prostate Cancer: Genes Related, Target Therapy and Prevention. International journal of molecular sciences. 2021,22(7). doi:10.3390/ijms22073753.
2. Mohler JL, Antonarakis ES, Armstrong AJ, D'Amico AV, Davis BJ, Dorff T et al. Prostate Cancer, Version 2.2019, NCCN Clinical Practice Guidelines in Oncology. Journal of the National Comprehensive Cancer Network : JNCCN. 2019,17(5):479-505. doi:10.6004/jnccn.2019.0023.
3. Cornford P, van den Bergh RCN, Briers E, Van den Broeck T, Cumberbatch MG, De Santis M et al. EAU-EANM-ESTRO-ESUR-SIOG Guidelines on Prostate Cancer. Part II-2020 Update: Treatment of Relapsing and Metastatic Prostate Cancer. European urology. 2021,79(2):263-82. doi:10.1016/j.eururo.2020.09.046.
4. Ge R, Wang Z, Montironi R, Jiang Z, Cheng M, Santoni M et al. Epigenetic modulations and lineage plasticity in advanced prostate cancer. Annals of oncology : official journal of the European Society for Medical Oncology. 2020,31(4):470-9. doi:10.1016/j.annonc.2020.02.002.
5. Matsumoto K, Niwa N, Hattori S, Takeda T, Morita S, Kosaka T et al. Establishment of the optimal follow-up schedule after radical prostatectomy. Urologic oncology. 2018,36(7):341.e9-.e14. doi:10.1016/j.urolonc.2018.04.003.
6. Ward JF, Blute ML, Slezak J, Bergstralh EJ, Zincke H. The long-term clinical impact of biochemical recurrence of prostate cancer 5 or more years after radical prostatectomy. The Journal of urology. 2003,170(5):1872-6. doi:10.1097/01.ju.0000091876.13656.2e.
7. Paller CJ, Antonarakis ES. Management of biochemically recurrent prostate cancer after local therapy: evolving standards of care and new directions. Clinical advances in hematology & oncology : H&O. 2013,11(1):14-23.
8. Bingle L, Brown NJ, Lewis CE. The role of tumour-associated macrophages in tumour progression: implications for new anticancer therapies. The Journal of pathology. 2002,196(3):254-65.

doi:10.1002/path.1027.

9. Gollapudi K, Galet C, Grogan T, Zhang H, Said JW, Huang J et al. Association between tumor-associated macrophage infiltration, high grade prostate cancer, and biochemical recurrence after radical prostatectomy. American journal of cancer research. 2013,3(5):523-9.
10. Hu W, Qian Y, Yu F, Liu W, Wu Y, Fang X et al. Alternatively activated macrophages are associated with metastasis and poor prognosis in prostate adenocarcinoma. Oncol Lett. 2015,10(3):1390-6. doi:10.3892/ol.2015.3400.
11. Chanmee T, Ontong P, Konno K, Itano N. Tumor-associated macrophages as major players in the tumor microenvironment. Cancers. 2014,6(3):1670-90. doi:10.3390/cancers6031670.
12. Karan D, Holzbeierlein J, Thrasher JB. Macrophage inhibitory cytokine-1: possible bridge molecule of inflammation and prostate cancer. Cancer research. 2009,69(1):2-5. doi:10.1158/0008-5472.Can-08-1230.
13. Izumi K, Mizokami A. Suppressive Role of Androgen/Androgen Receptor Signaling via Chemokines on Prostate Cancer Cells. Journal of clinical medicine. 2019,8(3). doi:10.3390/jcm8030354.
14. Ma J, Shayiti F, Ma J, Wei M, Hua T, Zhang R et al. Tumor-associated macrophage-derived CCL5 promotes chemotherapy resistance and metastasis in prostatic cancer. Cell biology international. 2021,45(10):2054-62. doi:10.1002/cbin.11630.
15. El-Kenawi A, Dominguez-Viqueira W, Liu M, Awasthi S, Abraham-Miranda J, Keske A et al. Macrophage-Derived Cholesterol Contributes to Therapeutic Resistance in Prostate Cancer. Cancer research. 2021,81(21):5477-90. doi:10.1158/0008-5472.Can-20-4028.
16. Schnepp PM, Shelley G, Dai J, Wakim N, Jiang H, Mizokami A et al. Single-Cell Transcriptomics Analysis Identifies Nuclear Protein 1 as a Regulator of Docetaxel Resistance in Prostate Cancer Cells. Molecular cancer research : MCR. 2020,18(9):1290-301. doi:10.1158/1541-7786.Mcr-20-0051.
17. Baures M, Puig Lombardi E, Di Martino D, Zeitouni W, Pacreau E, Dos Santos L et al. Transcriptomic Signature and Growth Factor Regulation of Castration-Tolerant Prostate Luminal Progenitor Cells. Cancers. 2022,14(15). doi:10.3390/cancers14153775.
18. Song P, Li W, Wu X, Qian Z, Ying J, Gao S et al. Integrated analysis of single-cell and bulk RNA-sequencing identifies a signature based on B cell marker genes to predict prognosis and immunotherapy response in lung adenocarcinoma. Cancer immunology, immunotherapy : CII. 2022,71(10):2341-54. doi:10.1007/s00262-022-03143-2.
19. Hao Y, Hao S, Andersen-Nissen E, Mauck WM, 3rd, Zheng S, Butler A et al. Integrated analysis of multimodal single-cell data. Cell. 2021,184(13):3573-87.e29. doi:10.1016/j.cell.2021.04.048.
20. Aran D, Looney AP, Liu L, Wu E, Fong V, Hsu A et al. Reference-based analysis of lung single-cell sequencing reveals a transitional profibrotic macrophage. Nature immunology. 2019,20(2):163-72. doi:10.1038/s41590-018-0276-y.
21. Gao J, Kwan PW, Shi D. Sparse kernel learning with LASSO and Bayesian inference algorithm. Neural networks : the official journal of the International Neural Network Society. 2010,23(2):257-64. doi:10.1016/j.neunet.2009.07.001.

22. Taylor JM. Random Survival Forests. Journal of thoracic oncology : official publication of the International Association for the Study of Lung Cancer. 2011,6(12):1974-5. doi:10.1097/JTO.0b013e318233d835.
23. Yoshihara K, Shahmoradgoli M, Martínez E, Vegesna R, Kim H, Torres-Garcia W et al. Inferring tumour purity and stromal and immune cell admixture from expression data. Nature communications. 2013,4:2612. doi:10.1038/ncomms3612.
24. Hänzelmann S, Castelo R, Guinney J. GSVA: gene set variation analysis for microarray and RNA-seq data. BMC bioinformatics. 2013,14:7. doi:10.1186/1471-2105-14-7.
25. Newman AM, Liu CL, Green MR, Gentles AJ, Feng W, Xu Y et al. Robust enumeration of cell subsets from tissue expression profiles. Nature methods. 2015,12(5):453-7. doi:10.1038/nmeth.3337.
26. Auslander N, Zhang G, Lee JS, Frederick DT, Miao B, Moll T et al. Robust prediction of response to immune checkpoint blockade therapy in metastatic melanoma. Nature medicine. 2018,24(10):1545-9. doi:10.1038/s41591-018-0157-9.
27. Hu J, Yu A, Othmane B, Qiu D, Li H, Li C et al. Siglec15 shapes a non-inflamed tumor microenvironment and predicts the molecular subtype in bladder cancer. Theranostics. 2021,11(7):3089-108. doi:10.7150/thno.53649.
28. Vickers AJ, Cronin AM, Elkin EB, Gonen M. Extensions to decision curve analysis, a novel method for evaluating diagnostic tests, prediction models and molecular markers. BMC Med Inform Decis Mak. 2008,8:53. doi:10.1186/1472-6947-8-53.
29. Kerr KF, Brown MD, Zhu K, Janes H. Assessing the Clinical Impact of Risk Prediction Models With Decision Curves: Guidance for Correct Interpretation and Appropriate Use. J Clin Oncol. 2016,34(21):2534-40. doi:10.1200/jco.2015.65.5654.
30. Kim K, Kim HS, Kim JY, Jung H, Sun JM, Ahn JS et al. Predicting clinical benefit of immunotherapy by antigenic or functional mutations affecting tumour immunogenicity. Nature communications. 2020,11(1):951. doi:10.1038/s41467-020-14562-z.
31. Majera D, Skrott Z, Bouchal J, Bartkova J, Simkova D, Gachechiladze M et al. Targeting genotoxic and proteotoxic stress-response pathways in human prostate cancer by clinically available PARP inhibitors, vorinostat and disulfiram. The Prostate. 2019,79(4):352-62. doi:10.1002/pros.23741.
32. Carbonetti G, Converso C, Clement T, Wang C, Trotman LC, Ojima I et al. Docetaxel/cabazitaxel and fatty acid binding protein 5 inhibitors produce synergistic inhibition of prostate cancer growth. The Prostate. 2020,80(1):88-98. doi:10.1002/pros.23921.
33. Pittet MJ, Michielin O, Migliorini D. Clinical relevance of tumour-associated macrophages. Nature reviews Clinical oncology. 2022,19(6):402-21. doi:10.1038/s41571-022-00620-6.
34. Han IH, Song HO, Ryu JS. IL-6 produced by prostate epithelial cells stimulated with Trichomonas vaginalis promotes proliferation of prostate cancer cells by inducing M2 polarization of THP-1-derived macrophages. PLoS neglected tropical diseases. 2020,14(3):e0008126. doi:10.1371/journal.pntd.0008126.

35. Nonomura N, Takayama H, Nakayama M, Nakai Y, Kawashima A, Mukai M et al. Infiltration of tumour-associated macrophages in prostate biopsy specimens is predictive of disease progression after hormonal therapy for prostate cancer. BJU international. 2011,107(12):1918-22. doi:10.1111/j.1464-410X.2010.09804.x.
36. Cioni B, Zaalberg A, van Beijnum JR, Melis MHM, van Burgsteden J, Muraro MJ et al. Androgen receptor signalling in macrophages promotes TREM-1-mediated prostate cancer cell line migration and invasion. Nature communications. 2020,11(1):4498. doi:10.1038/s41467-020-18313-y.
37. Yu S, Yang R, Xu T, Li X, Wu S, Zhang J. Cancer-associated fibroblasts-derived FMO2 as a biomarker of macrophage infiltration and prognosis in epithelial ovarian cancer. Gynecologic oncology. 2022. doi:10.1016/j.ygyno.2022.09.003.
38. Zhang C, Liu H, Tan Y, Xu Y, Li Y, Tong S et al. MS4A6A is a new prognostic biomarker produced by macrophages in glioma patients. Frontiers in immunology. 2022,13:865020. doi:10.3389/fimmu.2022.865020.
39. Truong M, Frye T, Messing E, Miyamoto H. Historical and contemporary perspectives on cribriform morphology in prostate cancer. Nature reviews Urology. 2018,15(8):475-82. doi:10.1038/s41585-018-0013-1.
40. Albertsen PC. Prostate cancer screening and treatment: where have we come from and where are we going? BJU international. 2020,126(2):218-24. doi:10.1111/bju.15153.
41. Tyekucheva S, Bowden M, Bango C, Giunchi F, Huang Y, Zhou C et al. Stromal and epithelial transcriptional map of initiation progression and metastatic potential of human prostate cancer. Nature communications. 2017,8(1):420. doi:10.1038/s41467-017-00460-4.
42. Wong RL, Yu EY. Refining Immuno-Oncology Approaches in Metastatic Prostate Cancer: Transcending Current Limitations. Current treatment options in oncology. 2021,22(2):13. doi:10.1007/s11864-020-00808-x.
43. Zhao SJ, Kong FQ, Jie J, Li Q, Liu H, Xu AD et al. Macrophage MSR1 promotes BMSC osteogenic differentiation and M2-like polarization by activating PI3K/AKT/GSK3β/β-catenin pathway. Theranostics. 2020,10(1):17-35. doi:10.7150/thno.36930.
44. Wang S, Liu R, Yu Q, Dong L, Bi Y, Liu G. Metabolic reprogramming of macrophages during infections and cancer. Cancer Lett. 2019,452:14-22. doi:10.1016/j.canlet.2019.03.015.
45. Mantovani A, Marchesi F, Malesci A, Laghi L, Allavena P. Tumour-associated macrophages as treatment targets in oncology. Nature reviews Clinical oncology. 2017,14(7):399-416. doi:10.1038/nrclinonc.2016.217.
46. Andersen LB, Nørgaard M, Rasmussen M, Fredsøe J, Borre M, Ulhøi BP et al. Immune cell analyses of the tumor microenvironment in prostate cancer highlight infiltrating regulatory T cells and macrophages as adverse prognostic factors. The Journal of pathology. 2021,255(2):155-65. doi:10.1002/path.5757.
47. Garrido-Martin EM, Mellows TWP, Clarke J, Ganesan AP, Wood O, Cazaly A et al. M1(hot) tumor-associated macrophages boost tissue-resident memory T cells infiltration and survival in human

lung cancer. Journal for immunotherapy of cancer. 2020,8(2). doi:10.1136/jitc-2020-000778.

48. Japp AS, Kursunel MA, Meier S, Mälzer JN, Li X, Rahman NA et al. Dysfunction of PSA-specific CD8+ T cells in prostate cancer patients correlates with CD38 and Tim-3 expression. Cancer immunology, immunotherapy : CII. 2015,64(11):1487-94. doi:10.1007/s00262-015-1752-y.
49. Piao Y, Jin X. Analysis of Tim-3 as a therapeutic target in prostate cancer. Tumour biology : the journal of the International Society for Oncodevelopmental Biology and Medicine. 2017,39(7):1010428317716628. doi:10.1177/1010428317716628.
50. Chen L, Flies DB. Molecular mechanisms of T cell co-stimulation and co-inhibition. Nature reviews Immunology. 2013,13(4):227-42. doi:10.1038/nri3405.
51. Jafari S, Molavi O, Kahroba H, Hejazi MS, Maleki-Dizaji N, Barghi S et al. Clinical application of immune checkpoints in targeted immunotherapy of prostate cancer. Cellular and molecular life sciences : CMLS. 2020,77(19):3693-710. doi:10.1007/s00018-020-03459-1.
52. Zhou J, Lai Y, Peng S, Tang C, Chen Y, Li L et al. Comprehensive analysis of TP53 and SPOP mutations and their impact on survival in metastatic prostate cancer. Front Oncol. 2022,12:957404. doi:10.3389/fonc.2022.957404.
53. Stopsack KH, Nandakumar S, Wibmer AG, Haywood S, Weg ES, Barnett ES et al. Oncogenic Genomic Alterations, Clinical Phenotypes, and Outcomes in Metastatic Castration-Sensitive Prostate Cancer. Clinical cancer research : an official journal of the American Association for Cancer Research. 2020,26(13):3230-8. doi:10.1158/1078-0432.Ccr-20-0168.
54. Liu Z, Guo H, Zhu Y, Xia Y, Cui J, Shi K et al. TP53 alterations of hormone-naïve prostate cancer in the Chinese population. Prostate cancer and prostatic diseases. 2021,24(2):482-91. doi:10.1038/s41391-020-00302-3.
55. Blagih J, Buck MD, Vousden KH. p53, cancer and the immune response. Journal of cell science. 2020,133(5). doi:10.1242/jcs.237453.
56. Bezzi M, Seitzer N, Ishikawa T, Reschke M, Chen M, Wang G et al. Diverse genetic-driven immune landscapes dictate tumor progression through distinct mechanisms. Nature medicine. 2018,24(2):165-75. doi:10.1038/nm.4463.
57. Dréan A, Rosenberg S, Lejeune FX, Goli L, Nadaradjane AA, Guehennec J et al. ATP binding cassette (ABC) transporters: expression and clinical value in glioblastoma. Journal of neuro-oncology. 2018,138(3):479-86. doi:10.1007/s11060-018-2819-3.
58. Le DT, Uram JN, Wang H, Bartlett BR, Kemberling H, Eyring AD et al. PD-1 Blockade in Tumors with Mismatch-Repair Deficiency. The New England journal of medicine. 2015,372(26):2509-20. doi:10.1056/NEJMoa1500596.
59. Hellmann MD, Nathanson T, Rizvi H, Creelan BC, Sanchez-Vega F, Ahuja A et al. Genomic Features of Response to Combination Immunotherapy in Patients with Advanced Non-Small-Cell Lung Cancer. Cancer cell. 2018,33(5):843-52.e4. doi:10.1016/j.ccell.2018.03.018.
60. Wood MA, Weeder BR, David JK, Nellore A, Thompson RF. Burden of tumor mutations, neoepitopes, and other variants are weak predictors of cancer immunotherapy response and overall survival.

Genome medicine. 2020,12(1):33. doi:10.1186/s13073-020-00729-2.

61. Barroso-Sousa R, Keenan TE, Pernas S, Exman P, Jain E, Garrido-Castro AC et al. Tumor Mutational Burden and PTEN Alterations as Molecular Correlates of Response to PD-1/L1 Blockade in Metastatic Triple-Negative Breast Cancer. Clinical cancer research : an official journal of the American Association for Cancer Research. 2020,26(11):2565-72. doi:10.1158/1078-0432.Ccr-19-3507.
62. Sánchez C, Mercado A, Contreras HR, Carvajal VF, Salgado A, Huidobro C et al. Membrane translocation and activation of GnRH receptor sensitize prostate cancer cells to radiation. International journal of radiation biology. 2021,97(11):1555-62. doi:10.1080/09553002.2021.1980628.
63. Xue YN, Yu BB, Liu YN, Guo R, Li JL, Zhang LC et al. Zinc promotes prostate cancer cell chemosensitivity to paclitaxel by inhibiting epithelial-mesenchymal transition and inducing apoptosis. The Prostate. 2019,79(6):647-56. doi:10.1002/pros.23772.
64. Terrisse S, Karamouza E, Parker CC, Sartor AO, James ND, Pirrie S et al. Overall Survival in Men With Bone Metastases From Castration-Resistant Prostate Cancer Treated With Bone-Targeting Radioisotopes: A Meta-analysis of Individual Patient Data From Randomized Clinical Trials. JAMA Oncol. 2020,6(2):206-16. doi:10.1001/jamaoncol.2019.4097.
65. Sternberg CN, Castellano D, de Bono J, Fizazi K, Tombal B, Wülfing C et al. Efficacy and Safety of Cabazitaxel Versus Abiraterone or Enzalutamide in Older Patients with Metastatic Castration-resistant Prostate Cancer in the CARD Study. European urology. 2021,80(4):497-506. doi:10.1016/j.eururo.2021.06.021.
66. Elhasasna H, Khan R, Bhanumathy KK, Vizeacoumar FS, Walke P, Bautista M et al. A Drug Repurposing Screen Identifies Fludarabine Phosphate as a Potential Therapeutic Agent for N-MYC Overexpressing Neuroendocrine Prostate Cancers. Cells. 2022,11(14). doi:10.3390/cells11142246.
67. Zhao Q, Luo YF, Tian M, Xiao YL, Cai HR, Li H. Activating transcription factor 3 involved in Pseudomonas aeruginosa PAO1-induced macrophage senescence. Molecular immunology. 2021,133:122-7. doi:10.1016/j.molimm.2021.02.016.
68. Middleton JD, Fehlman J, Sivakumar S, Stover DG, Hai T. Stress-Inducible Gene Atf3 Dictates a Dichotomous Macrophage Activity in Chemotherapy-Enhanced Lung Colonization. International journal of molecular sciences. 2021,22(14). doi:10.3390/ijms22147356.
69. Wang Z, Xu D, Ding HF, Kim J, Zhang J, Hai T et al. Loss of ATF3 promotes Akt activation and prostate cancer development in a Pten knockout mouse model. Oncogene. 2015,34(38):4975-84. doi:10.1038/onc.2014.426.
70. Wang Z, Kim J, Teng Y, Ding HF, Zhang J, Hai T et al. Loss of ATF3 promotes hormone-induced prostate carcinogenesis and the emergence of CK5(+)CK8(+) epithelial cells. Oncogene. 2016,35(27):3555-64. doi:10.1038/onc.2015.417.

Figures

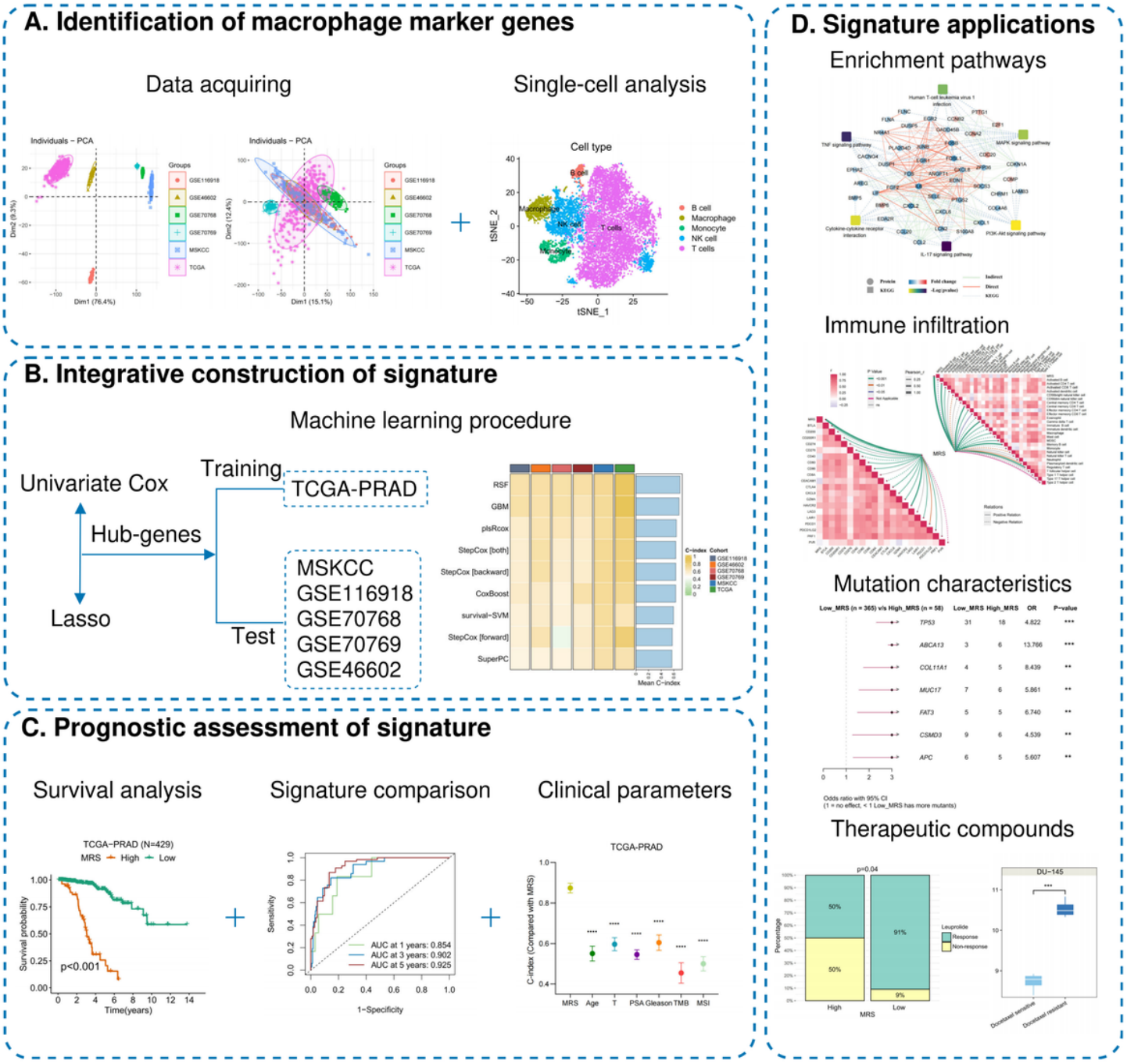

Figure 1

The workflow of the research.

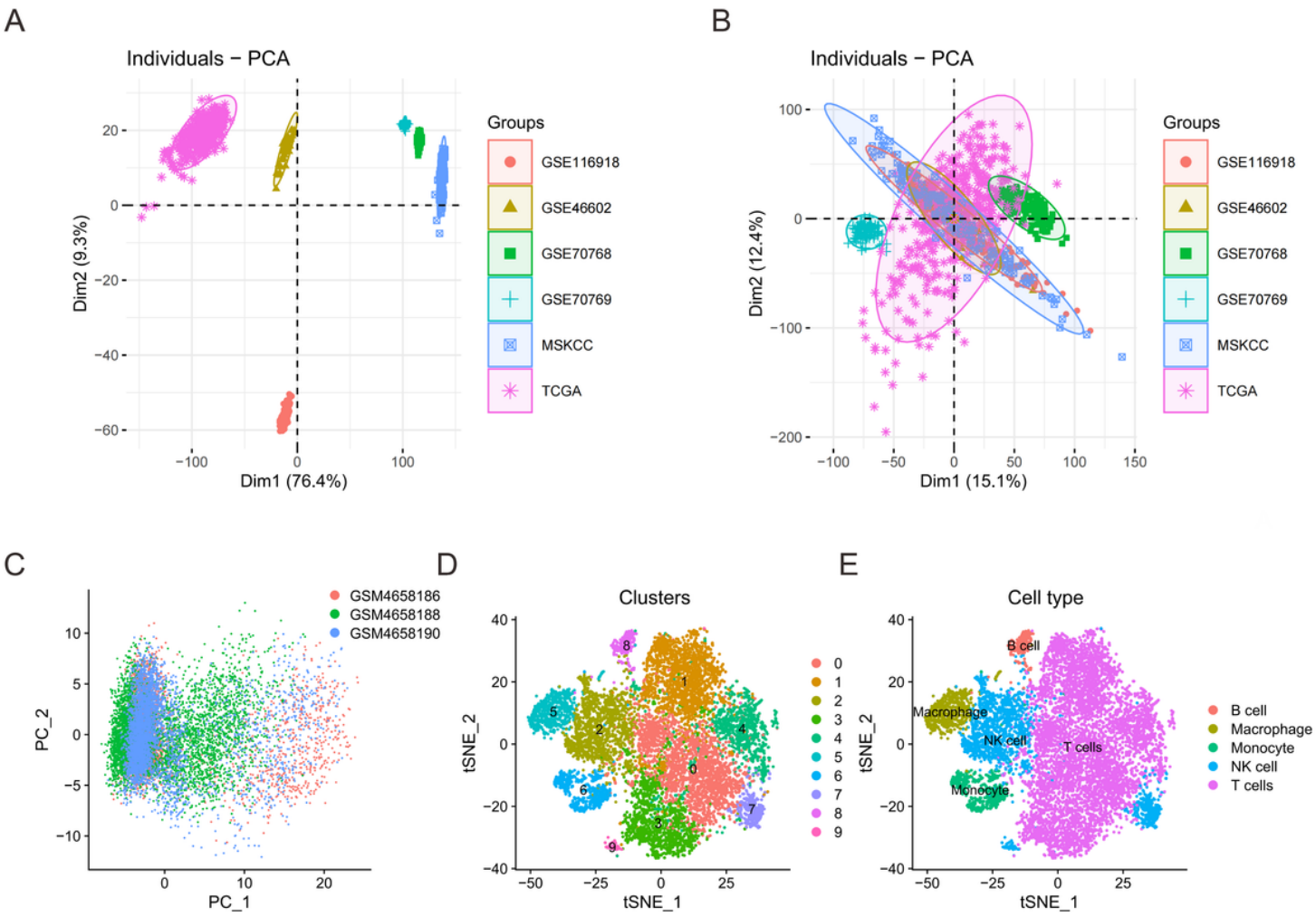

Figure 2

Identification and selection of macrophage marker genes in PCa. (**A, B**) The distribution of prostate cancer samples (TCGA-PRAD, MSKCC, GSE116918, GSE70768, GSE70769, and GSE46602) before and after removal of batch effects by principal component analysis. (**C**) PCa dimension reduction by scRNA-seq, Color depending on various samples. (**D**) Label colors according to various cell types. (**E**) Cluster annotation of cell types using standard markers.

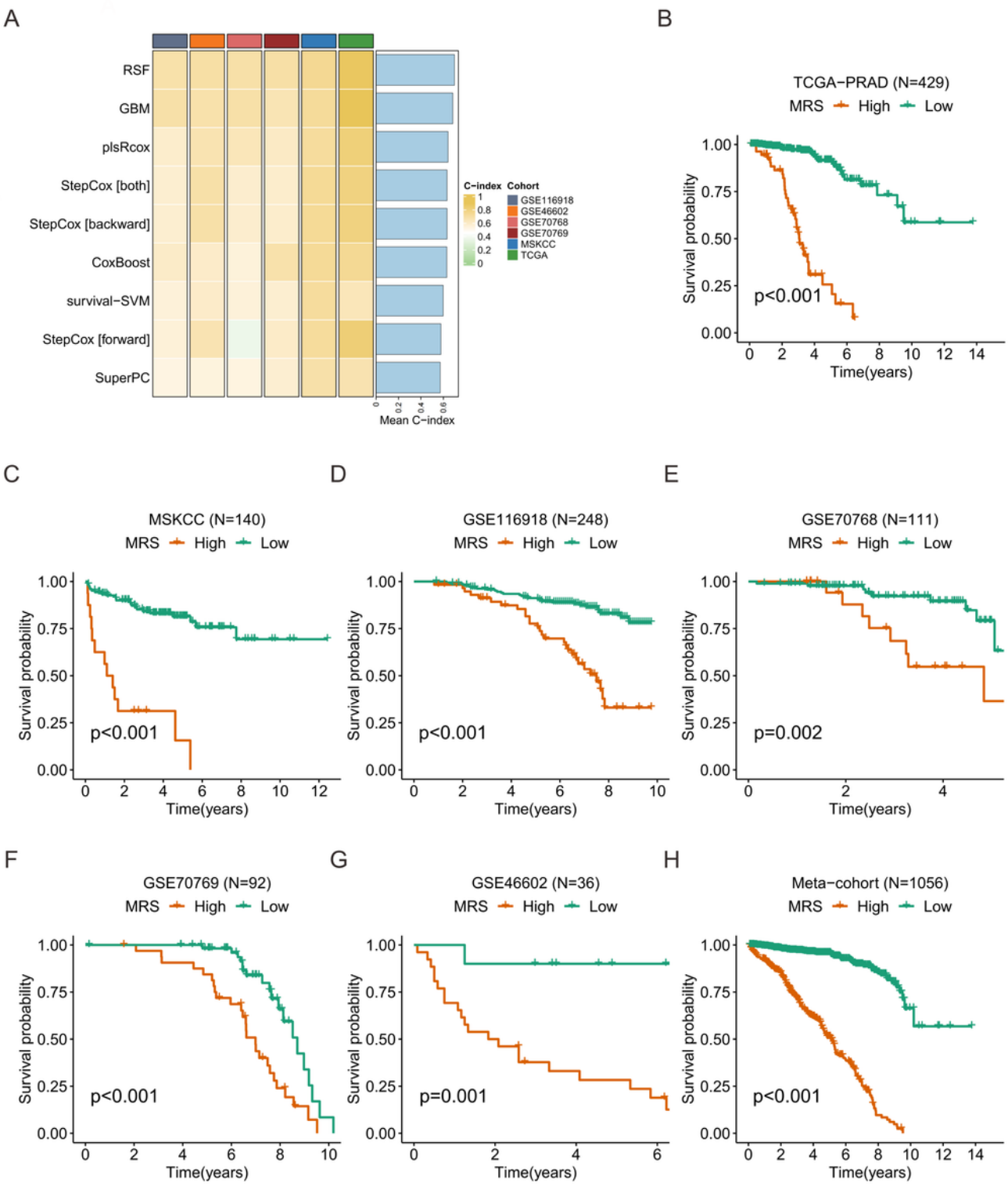

Figure 3

Construction of MRS model via the machine learning-based procedure. (**A**) A total of nine prediction models were developed through the LOOCV framework and the C-index was further calculated for each model across all validation datasets. Kaplan-Meier curves showed that patients with lower MRS scores had better RFS than the ones with higher MRS scores in the TCGA-PRAD (**B**), MSKCC(**C**), GSE116918(**D**), GSE70768(**E**), GSE70769(**F**), GSE46602(**G**), and meta-cohort(**H**).

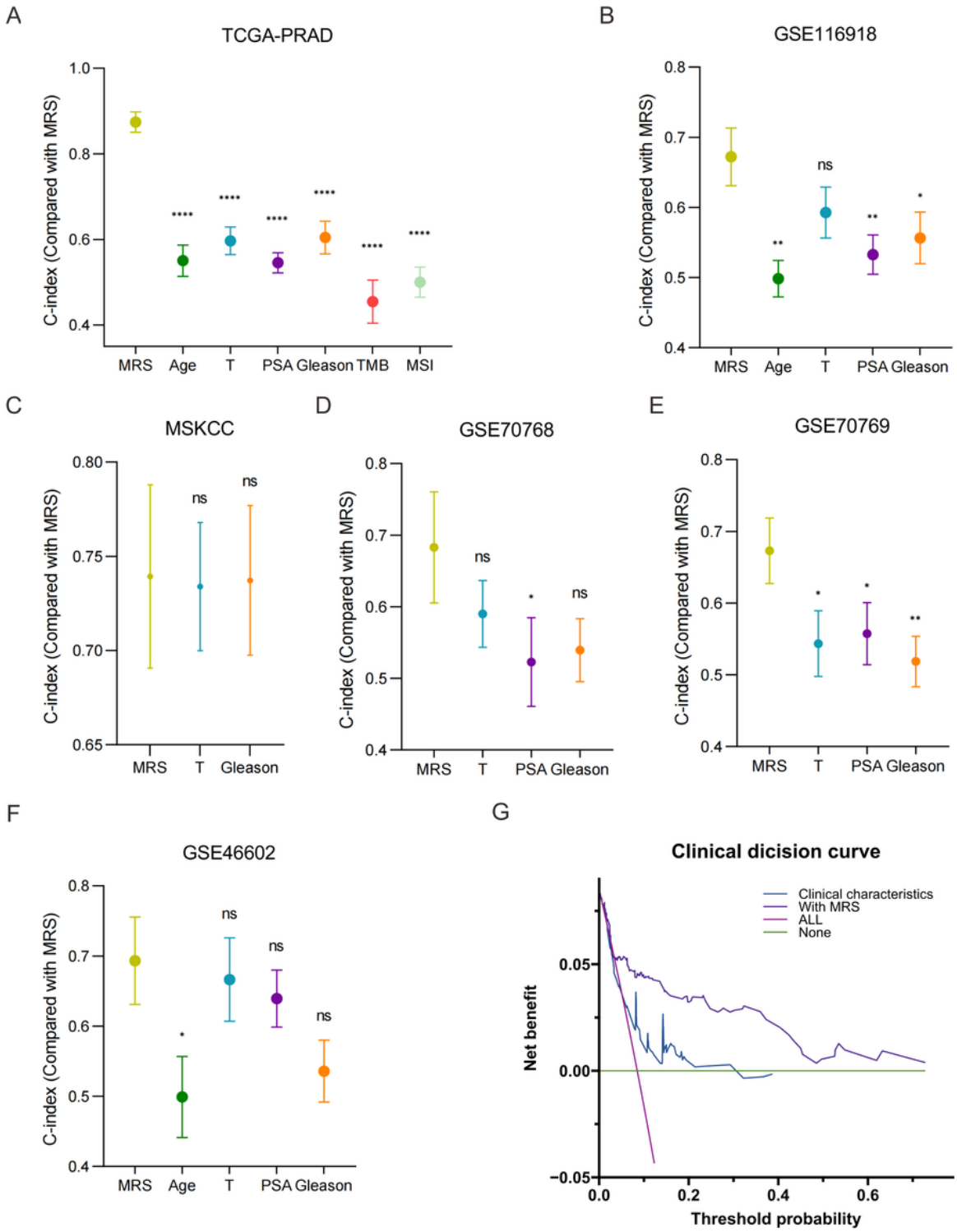

Figure 4

Evaluation of the MRS model. (**A-F**) The performance of MRS was compared with other clinical and molecular variables in predicting prognosis. (**G**) Comparisons of the clinical utility for the clinical variables and combined with MRS using decision curve in the entire TCGA dataset. *P < 0.05, **P < 0.01, ***P < 0.001, ****P < 0.0001, ns: no significance.

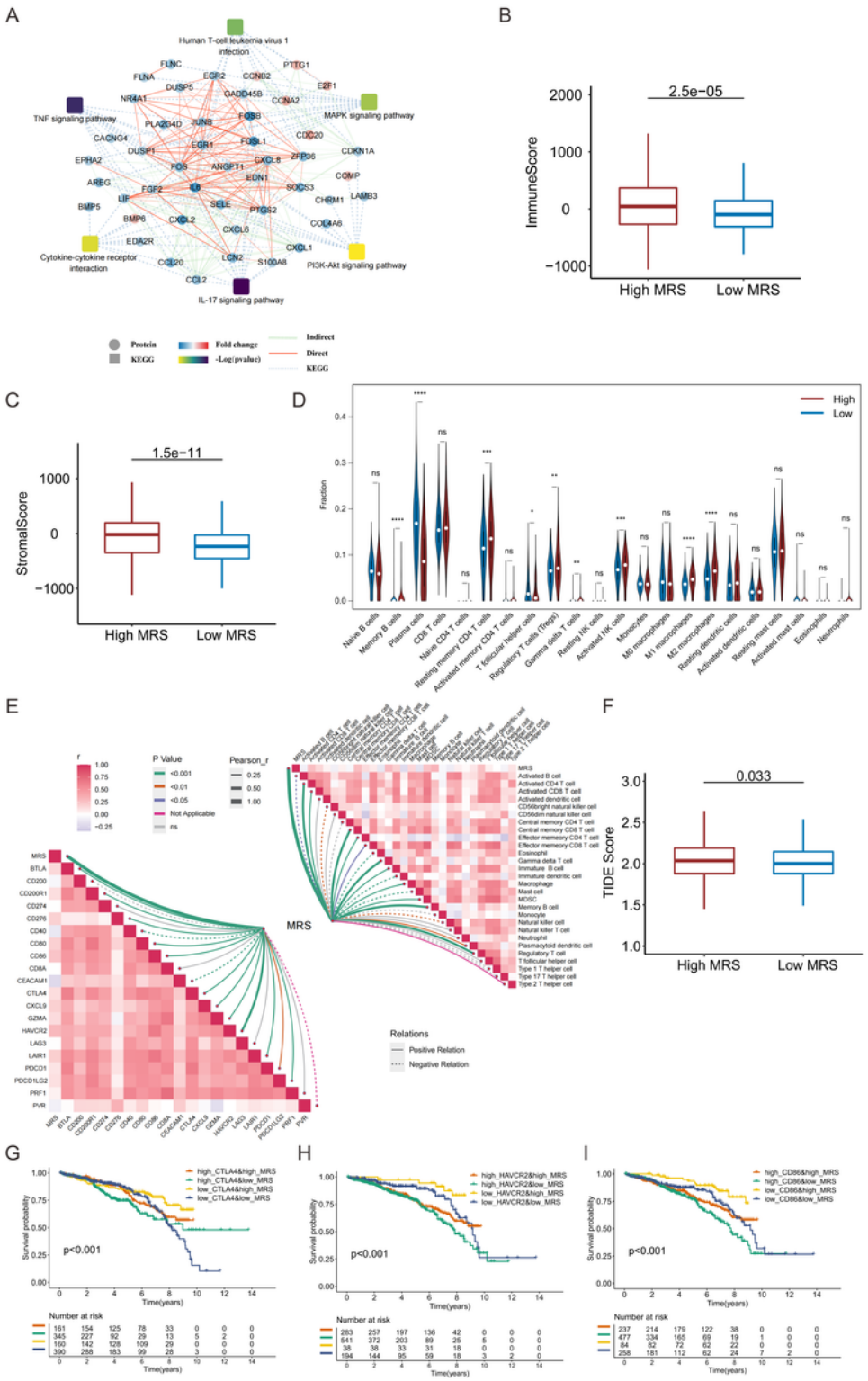

Figure 5

Immunological features in prostate cancer. (**A**) The diagram depicted the protein interactions of multiple immune-related pathways. The green backward slash lines represent indirect, the red solid lines represent direct, the grey dotted lines represent the KEGG pathway. Colour bars from red to blue represent the fold change in protein levels from increasing to decreasing. The significance of pathways represented by -log (pvalue) (limma test) was indicated as most significant in dark purple. (**B, C**) The box plots presented that

both immune score and stromal score are significantly correlated with MRS subtypes. (**D**) Comparison of 22 cellular levels inferred by CIBERSORT algorithm between high/low MRS groups in meta-cohort. (**E**) A correlation heatmap illustrated the relationships of MRS score with the immune infiltrating cells and inhibitory immune checkpoints. (**F**) The differences in TIDE score between two MRS subgroups. KM curve of four subgroups stratified according to the MRS scores and expression of inhibitory immune checkpoints for CTLA4 (**G**), HAVCR2 (**H**), and CD86 (**I**), respectively. *P < 0.05, **P < 0.01, ***P < 0.001, ****P < 0.0001, ns: no significance.

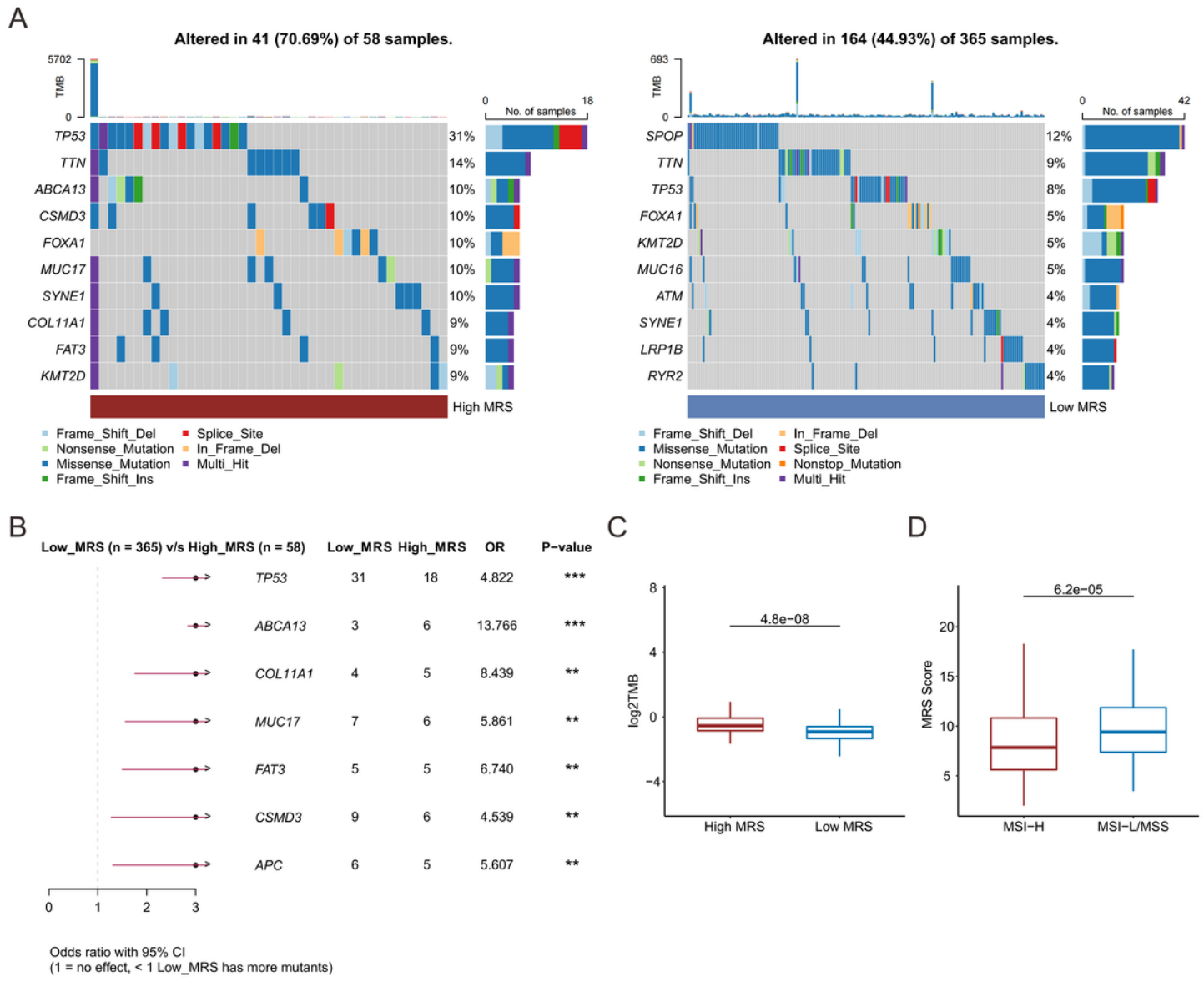

Figure 6

Landscape of somatic mutations. (**A**) The top 10 mutated genes are in the high MRS and low MRS score groups. (**B**) The somatic mutations were compared between the high/low MRS score groups. (**C**) The relationship between TMB and MRS scores in PCa patients. (**D**) Comparison of the MRS score between MSI-L/MSS and MSI-H group. *P < 0.05, **P < 0.01, ***P < 0.001, ****P < 0.0001, ns: no significance.

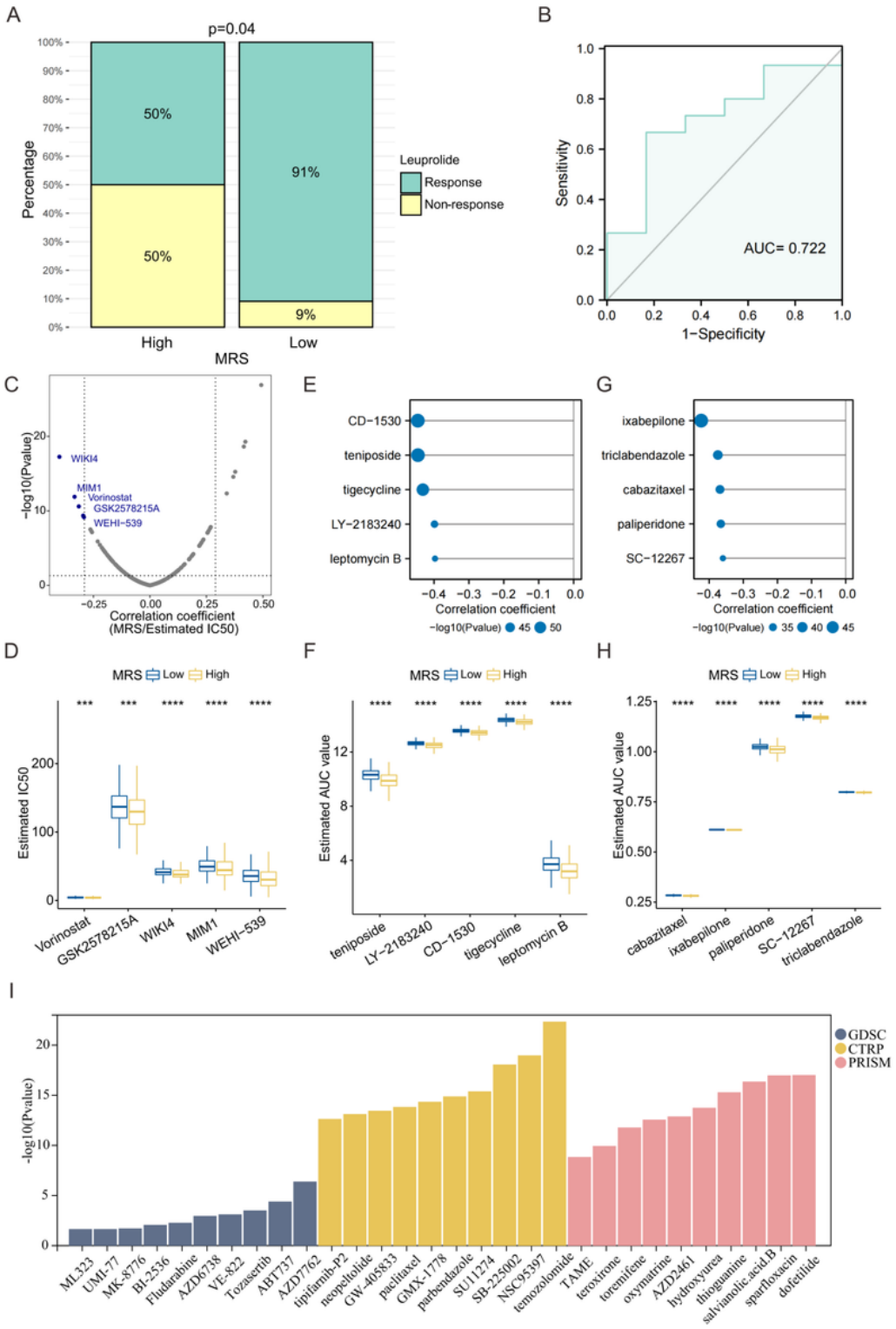

Figure 7

MRS predicted therapeutic response for PCa patients. (**A**) Differences in response rates between the high MRS and the low MRS score group concerning Leuprolide-based ACT. (**B**) ROC curves of MRS predict the efficacy of leuprolide in TCGA. For the GDSC database, volcano plot (**C**) and box plot (**D**) of Pearson's correlations and significance between MRS scores and estimated IC50 values, and blue points being significantly negatively correlated ($p < 0.05$, $r < -0.29$). (**E, G**) The AUC values of compounds in CTRP and

PRISM were estimated for each PRAD sample and Pearson correlation was performed between MRS scores and estimated AUC values, and the five compounds with the highest negative correlation coefficients were shown on dotted line plots (CTRP: r < -0.39, PRISM: r < - 0.35). (**F, H**) All estimated AUC values for these compounds were significantly lower in the MRS high group. ***P < 0.001, ****P < 0.0001. (**I**) Barplot showed drugs with differences in pharmacological value between high and low MRS scores in the GDSC (blue), CTRP (yellow), and PRISM (pink) databases, where columns represent p values and rows represent drugs. *P < 0.05, **P < 0.01, ***P < 0.001, ****P < 0.0001, ns: no significance.

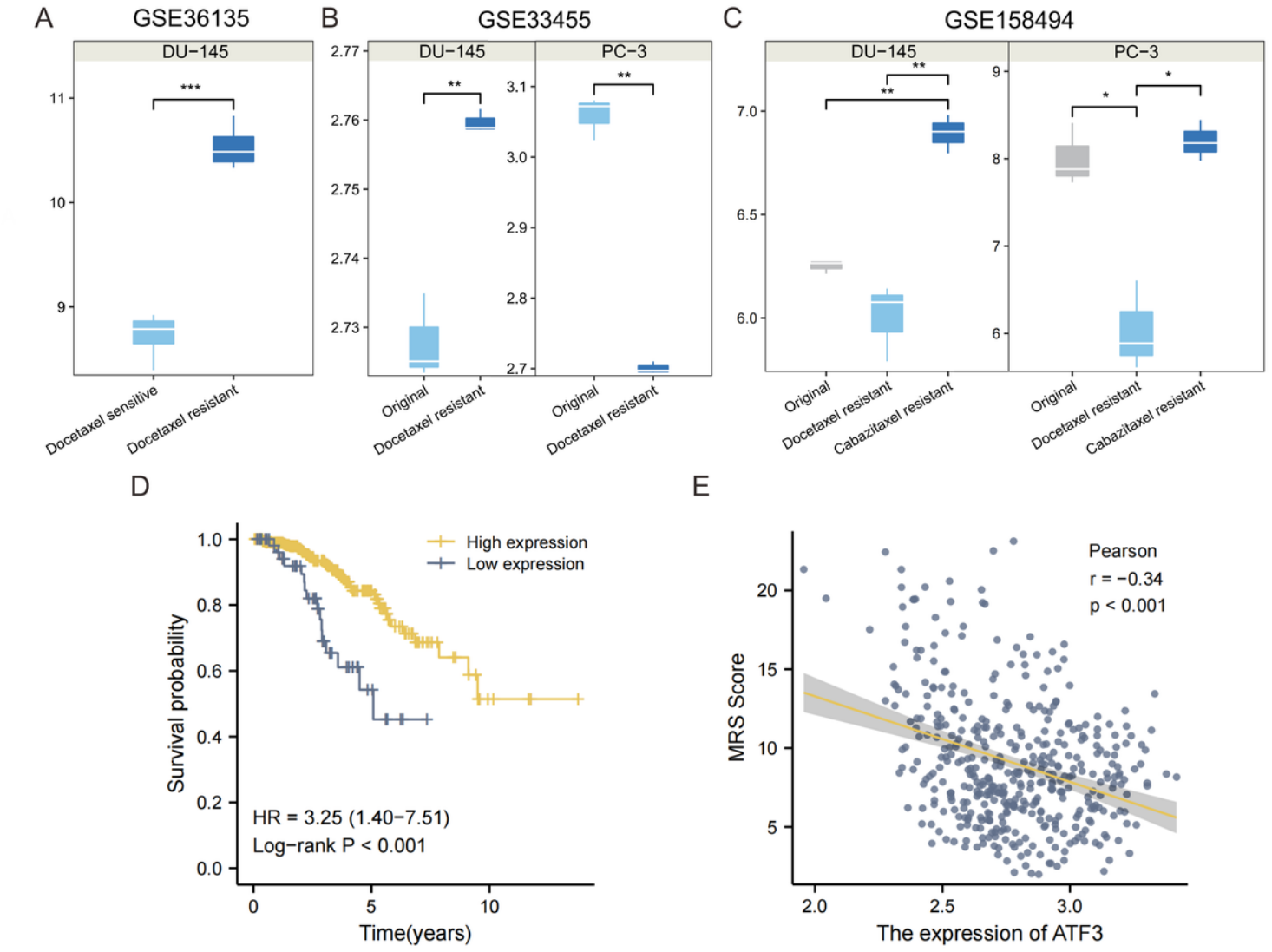

Figure 8

Molecular comparison in prostate cancer cell lines. (**A**) Boxplot compared abnormal ATF3 expression between docetaxel-resistant and docetaxel-sensitive DU-145 cells in GSE36135. The differences of ATF3 expression between original and docetaxel (or cabazitaxel) resistant DU-145 (or PC-3) cell lines in the GSE33455 (**B**) and GSE158494 (**C**) databases, respectively. *P < 0.05, **P < 0.01, ***P < 0.001, ****P < 0.0001, ns: no significance. (**D**) KM survival curves showed the difference in RFS between the two groups

with high and low ATF3 expression. (**E**) In the TCGA cohort, ATF3 displayed a significant negative correlation with MRS scores.

Supplementary Files

This is a list of supplementary files associated with this preprint. Click to download.

- Supplementaryfile.docx
- figS1.tif
- figS2.tif
- figS3.tif